Catalysis Today 141 (2009) 254–259

Contents lists available at ScienceDirect

Catalysis Today

journal homepage: www.elsevier.com/locate/cattod

Ammoxidation of propane over Fe-zeolites: Effect of reaction variables and catalyst composition and structure

Roman Bulánek [a,*], Kateřina Raabová [a], Gabriela Košová-Kučerová [b], Libor Čapek [a]

[a] Department of Physical Chemistry, Faculty of Chemical Technology, University of Pardubice, Nam. Čs. legií 565, CZ-532 10 Pardubice, Czech Republic
[b] Department of Chemistry and Biochemistry, University of Munich (LMU), Butenandtstrasse 11 (E), 81377 Munich, Germany

ARTICLE INFO

Article history:
Available online 9 June 2008

Keywords:
Catalysis
Ammoxidation
Propane
Fe-silicalite

ABSTRACT

A series of Fe-silicalite catalysts with tailored dispersion of Fe sites ranging from almost exclusively isolated Fe ions via oligonuclear cluster to Fe_2O_3 particles were characterized by UV–vis and ESR spectroscopy. The same catalysts were tested in the direct ammoxidation of propane at 540 °C in the mixture of molecular oxygen and nitrous oxide. Obtained catalytic results were compared with spectroscopic characterization. The presented results clearly showed that the changes in the catalytic performance of investigated catalysts are in correspondence with results of spectroscopic characterization. Acrylonitrile is produced on extra-framework Fe species exclusively generated by hydrolysis of framework Si–O–Fe bonds both during reaction and by steaming in water vapor at 600 °C as was evidenced by UV–vis and ESR spectroscopy. We supposed that active sites have character of well isolated extra-framework sites with tetrahedral coordination characterized by UV bands below 300 nm and ESR signals with *g* higher than 5.

© 2008 Elsevier B.V. All rights reserved.

1. Introduction

Acrylonitrile (ACN) is a major chemical commodity used in a variety of applications [1], mainly as a raw material in the manufacture of polyacrylonitrile fibers, plastics, adiponitrile, acrylamide and nitrile rubber. More than 4.5 millions tons of acrylonitrile (90% overall production) are produced worldwide by SOHIO Corp. which invented a process based on ammoxidation of propene at 380 °C over mixed oxide U–Sb–O or Mo–Bi–O [2]. The lower cost of propane relative to propene and the worldwide propene deficiency due to its increasing consumption for polymerization provide an incentive for the development of a process for direct conversion of propane to acrylonitrile. The various processes for the conversion of propane to ACN have been investigated. Direct catalytic ammoxidation of propane to acrylonitrile can be carried out on mixed-oxide catalysts based on V-Sb [3,4], V-Bi [5,6], V-Ga [7–10] and Sb-Ga [4] or V-Mo [4]. Up to this day, no catalytic system exhibits parameters sufficient for commercial application. This is the reason why the attention in the field of activation and conversion of propane to acrylonitrile turns also to the other catalytic systems. Metal ions in molecular sieves might be a promising new type of catalysts for ammoxidation of propane. Considering the mechanistic point of view of the ammoxidation reaction of alkanes, perspective catalysts can be expected those showing the activity in oxidative dehydrogenation of alkanes to corresponding olefins. Metal ions, metal oxo-complexes and nanooxidic clusters embedded in the inner volume of pore system of micro- and mesoporous silicas appear to be the promising system for conversion of low alkanes to more valuable chemicals.

In 1997, Li and Armor [11–16] reported direct selective ammoxidation of ethane to acetonitrile (AcCN) over Co loaded high silica zeolites with MFI, BEA and NU-87 topologies. Derouane-Abd Hamid et al. [17,18] reported catalytic activity of Ga-modified MFI zeolites prepared by ion exchange of gallium from gallium nitrate solution in direct ammoxidation of propane to acrylonitrile leading to acrylonitrile yield about 20%. In last 5 years, unique activity of steamed Fe-MFI zeolites with traces of iron was reported in propane oxidation to propene with nitrous oxide [19–28]. In 2005, Perez-Ramirez et al. reported high activity of steam-activated Fe-silicalite with 6800 ppm of Fe ions in ammoxidation of propane [29]. They reported synergetic effect of N_2O and O_2 which led to acrylonitrile yield up to 10.5%, while propane ammoxidation by N_2O or O_2 reached yields of acrylonitrile below 5%. Unfortunately, these interesting yields of acrylonitrile are accompanied by relatively high amount of acetonitrile with yield up to 13.4%. Nevertheless, these results open new perspectives to improve the performance of alkane ammoxidation reaction.

---

* Corresponding author.
E-mail address: Roman.Bulanek@upce.cz (R. Bulánek).

0920-5861/$ – see front matter © 2008 Elsevier B.V. All rights reserved.
doi:10.1016/j.cattod.2008.03.035

Recently, we reported catalytic performance of various Fe-zeolites differing in Fe loading, framework composition and methods of preparation [30]. We have found that introduction of Fe ions into silicalite matrix by post-synthesis modification does not lead to an active catalyst for propane ammoxidation. In addition, our results indicate that the presence of aluminum atoms in the framework is disadvantageous for propane ammoxidation, in contrast to propane oxidative dehydrogenation by nitrous oxide, due to decomposition of acrylonitrile on strong acidic sites.

In summary, a novel promising catalytic system for direct propane ammoxidation must be explored between zeolite matrices in very high silica or pure silica form of zeolites without strong acidic protons on the surface with special type of Fe complex arising from Fe ions originally in the framework position of ferrosilicates. In this paper, we study (i) effect of Fe ions distribution after various pretreatments, (ii) effect of concentration of N_2O in reaction mixture and (iii) effect of time-on-stream (TOS) on the catalytic behavior of aluminum-free ferrosilicates.

2. Experimental

A set of Fe-silicalite catalysts with Fe species (ranging in Si/Fe ratio from 90 to 875) introduced during zeolite synthesis were investigated. Fe-silicalite was prepared by hydrothermal synthesis from mixture, which molar composition was as follows:$1SiO_2$, $10H_2O$, 0.4TPAOH, xFe$(NO_3)_3$, 2.6EtOH. (x = 0.0021–0.01). Synthesis was done in the autoclave with stirring at 170 °C for 72 h. The sol was filtered, washed with de-ionized water, dried at 120 °C for 2 h and calcined in the stream of dry oxygen at 540 °C for 8 h to remove the template.

The NH_4 form of the zeolites was prepared by ion exchange of the calcined material with 1 M solution of NH_4NO_3 at 50 °C overnight. Resulting sol was washed with de-ionized water and dried at 120 °C overnight. The final catalysts were calcined in dry oxygen at 540 °C (denoted as C) or steamed (10 vol.% of water vapor in nitrogen) at 600 °C (denoted as HT). The elemental analysis of catalysts was done by inductively coupled plasma optical emission spectroscopy (GBC Integra XL, Australia) after zeolite dissolution. The samples are labeled as follows: iron-zeolite structure, iron concentration in ppm, type of pretreatment.

ESR spectra of Fe^{3+} ions were monitored in the X-band region (λ = 3.2 cm) on the ESR spectrometer (ERS-220, Germany). Spectra were recorded at 298 K in the region of 23–523 mT. Before the measurements the samples were pretreated in reactor for 2 h at 450 °C under dynamic vacuum. Mn^{2+} ions in a solid matrix were used as an internal standard.

UV–vis spectra of Fe species were monitored on UV–vis spectrometer GBS CINTRA 303 equipped with a diffuse reflectance attachment with an integrating sphere coated with $BaSO_4$ and $BaSO_4$ as a reference. The absorption intensity was expressed using the Schuster–Kubelka–Munk equation.

Ammoxidation of propane was carried out in a fixed bed through-flow microreactor at atmospheric pressure. The amount of catalyst used was 0.2 g diluted by 1 cm^3 of inert silicon carbide. The total flow rate was 100 cm^3/min, the feed composition was 5 vol.% of propane, 5 vol.% of NH_3, 5 vol.% of O_2 and 0–6 vol.% of N_2O in helium. The reaction was measured at the temperature of 540 °C. The catalysts were pretreated in flow of oxygen for 1 h at 540 °C. Product gases were analyzed on-line by GC equipped with TCD and FID. Conversion, selectivity and yields were calculated on the basis of mass balance in dependence on the time of stream.

3. Results and discussion

3.1. Catalysts characterization

The DR UV–vis spectra of hydrated samples of calcined and steamed Fe catalyst are displayed in Fig. 1. In general, d–d transitions of Fe^{3+} are expected between 350 and 550 nm. However, they are symmetry and spin forbidden and therefore, extremely weak. Moreover, they can overlap with the tail of the low-energy charge transfer (CT) bands of oligomeric complexes. Therefore, the d–d transition bands can be visible only in the case of samples where Fe^{3+} ions are isolated and in perfect tetrahedral position. Indeed, the very weak bands can be observed in the visible region for the calcined samples (see inset in Fig. 1). Hence, interpretation of the spectra is focused on the intense Fe ← O charge transfer bands. It is well known that for Fe^{3+} ions two charge transfer bands corresponding to $t_1 \rightarrow t_2$ and $t_1 \rightarrow e$ transition can be detected. For isolated Fe^{3+} sites, they fall in the range of 200–300 nm. On the base of literature [31–34], CT bands at 215 and 249 nm were ascribed to tetrahedrally coordinated Fe ions incorporated in the framework of silicalite and CT band at 275 nm arises from isolated Fe^{3+} ions in octahedral coordination. It is generally accepted that increasing number of Fe–O–Fe bonds (and therefore increasing Fe_xO_y cluster size) led to shift of CT bands to higher wavelength. Thus, bands at 300–450 nm are assigned to small oligonuclear clusters inside the zeolite pores, bands above 450 nm are characteristic for Fe_2O_3 particles of different sizes. On

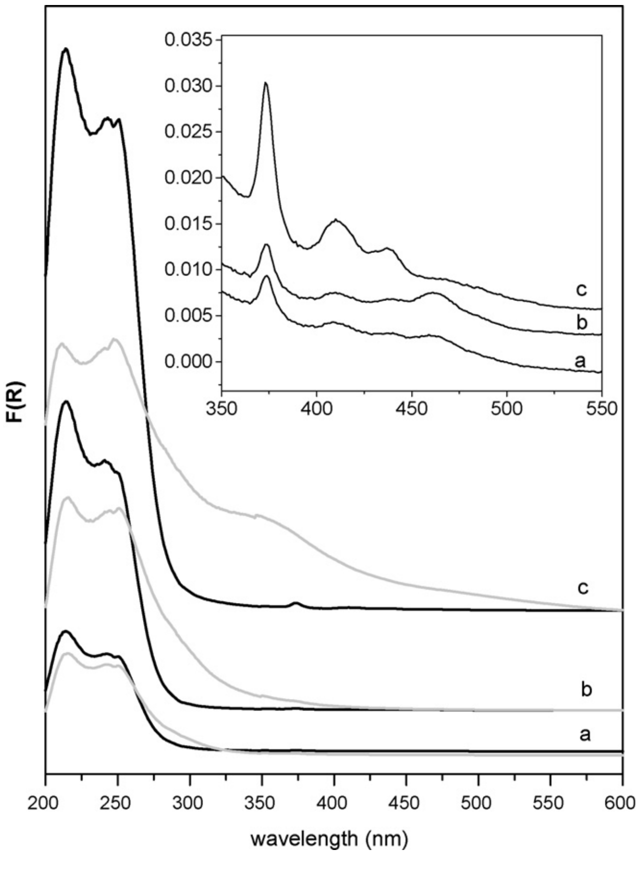

Fig. 1. DR UV–vis spectra of hydrated Fe-silicalite catalysts pretreated by calcination in flow of dry oxygen at 540 °C (black curves) and steam-treated in the flow of water vapor at 600 °C (gray curves). Curves a—Fe-sil-1000, curves b—Fe-sil-2500, curves c—Fe-sil-5000. Inset plot: the spectral region of d–d transitions of calcined Fe-silicalites.

the base of this assignment we can discuss our experimental spectra.

Fig. 1 clearly shows that the calcined Fe catalysts contained only isolated Fe sites mainly in the tetrahedral coordination. Intensity of the spectra at 275 nm is very low for calcined samples. It means that calcination of as-synthesized samples in dry oxygen at 540 °C is sufficiently mild pretreatment and Fe ion localization in the framework is preserved. Activation of Fe catalyst in the stream of water vapor at 600 °C led to extraction of Fe ions from framework positions to extra-framework sites by means of hydrolysis of Si–O–Fe bonds as is reflected by increasing of spectra intensity at higher wavelength and decreasing of bands intensity at 215 and 249 nm. This process leads to formation of various iron species, including isolated iron ions and oligonuclear species. With increasing Fe content the population of oligomeric clusters increases and in the case of Fe-silicalite with the highest Fe content, significant amount of Fe_2O_3 particles is present in the sample after steam pretreatment, as is reflected in the shoulder at 490 nm.

Distribution of Fe species and changes in the coordination environment of Fe ions were also investigated by ESR spectroscopy in both calcined and steamed samples of the investigated Fe catalysts. ESR spectroscopy is a sensitive method for investigation of the state of trivalent Fe ions. Several signals at $g \approx 2.0$, 4.3 and above 5 can be distinguished in the spectra of Fe silicates [35–38]. Signals at effective g-value of $g \approx 4.3$ have been assigned to the isolated Fe^{3+} ions in strong rhombic distortion of tetrahedral coordination in both framework and extra-framework sites. Signals with g-value above 5 were interpreted as Fe^{3+} ions in octahedral sites with strong axial distortion. In addition, a narrow and a broad signal at $g \approx 2$ can be discerned. These two contributions to signal at $g \approx 2$ arise from oxidic clusters of different sizes (broad and intense signal) and from well isolated Fe^{3+} sites of high symmetry, for which discrimination between tetrahedral and octahedral symmetries were not possible (less-intense and narrow signal). In Fig. 2, experimental ESR spectra of calcined and steamed samples are presented. In ESR spectra of calcined samples, signal at $g \approx 4.3$ is dominated. In addition, small signals at $g \approx 8.76$ are detected in the spectra of Fe-silicalites with Fe content higher than 1000 ppm. This is in agreement with the results of UV–vis spectroscopy, where only signals at 215 and 249 nm were detected in the calcined samples with small shoulder at 275 nm in the spectra of Fe-silicalites with higher Fe content, indicating the presence almost exclusively isolated Fe species. Pretreatment of samples in the stream of water vapor at 600 °C led to disappearance of original signals at $g \approx 4.3$ and 8.76 and formation of new signals at $g \approx 7.6$, 5.2 and 2.06. The intensity of broad signal at $g \approx 2.06$ increases with Fe content in the samples, no signal at $g \approx 2.06$ is detected for Fe-silicalite with 1000 ppm, whereas this signal dominates in the spectrum of Fe-silicalite with 5000 ppm of Fe. The behavior of ESR signals is in very good agreement with the results of UV–vis spectroscopy. In the samples with Fe content of 2500 and 5000 ppm, for which UV–vis spectra indicate the presence of a certain amount of oligomers and even some Fe_2O_3 particles (band and shoulder above 300 and 450 nm in the spectra reported in Fig. 1), the broad signal at $g \approx 2.06$ is pronounced.

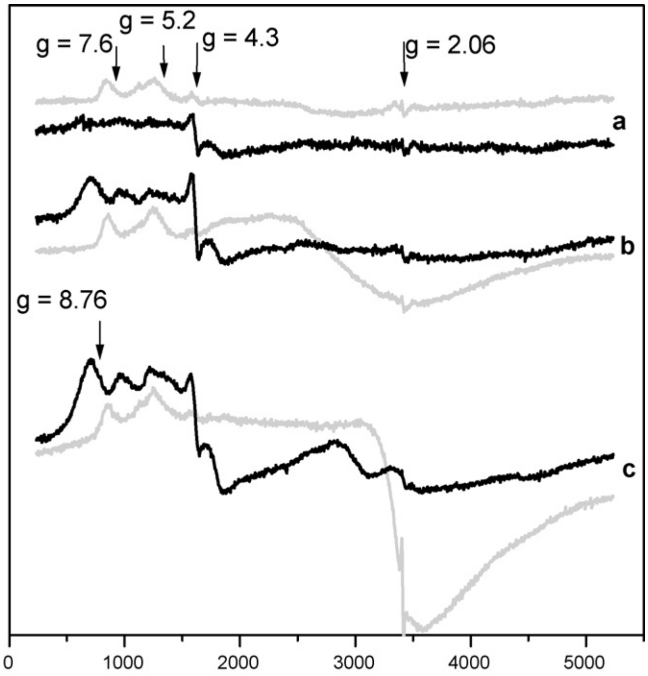

Fig. 2. Experimental ESR spectra of dehydrated Fe-silicalite catalysts measured at ambient temperature. Black curves—catalysts pretreated in the flow of dry oxygen at 540 °C, gray curves—catalysts steamed in the flow of water vapor at 600 °C. Curve a—Fe-sil-1000, curve b—Fe-sil-2500, curve c—Fe-sil-5000.

The results of spectroscopic characterization of Fe-silicalite catalysts show that the hydrothermally synthesized catalysts calcined in the dry oxygen have a Fe species mainly in the form of isolated mononuclear Fe ions. Steam activation of the catalysts led to massive migration of Fe ions, changes in the state and coordination of Fe species and their clustering leading to coexistence of isolated extra-framework Fe species and oligomeric complexes with low nuclearity. At sample with Fe content of 5000 ppm, steam-treatment led to the formation of small Fe_2O_3 nanoparticles. In the next part of article we will compare and discuss these spectroscopic results with catalytic behavior of investigated catalysts in ammoxidation of propane.

3.2. Reactivity tests

In the direct ammoxidation of propane, in the presence of oxygen and nitrous oxide mixture over Fe-silicalite catalysts, the product mixture consisted of propene, acrylonitrile, acetonitrile, and carbon oxides (CO_x). Traces of methane, ethane, ethene and HCN were also detected with selectivity not exceeding 3%. The initial catalytic performance (after 15 min of reaction run) of the investigated catalysts is summarized in Table 1. It is clearly seen that the activity and selectivity of catalysts are influenced not only by the content of iron, but also by the pretreatment. The conversion of propane increases with increasing content of iron from 6% for pure silicalite without iron to 54.5% for steamed Fe-silicalite with 5000 ppm of Fe and it is always higher for steamed catalysts in comparison with calcined ones. The selectivity to acrylonitrile and acetonitrile follows trends of conversion with exception of Fe-sil-

Table 1
The initial catalytic performance of the Fe-silicalite catalysts in propane ammoxidation

Catalyst	$X_{propane}$ (%)	Selectivity (%)				Yield (%)		
		C_3H_6	ACN	AcCN	CO_x	C_3H_6	ACN	AcCN
Sil-0	6.0	60.6	nd	nd	15.8	3.6	–	–
Fe-sil-1000-C	11.5	55.7	2.4	4.1	8.2	6.4	0.3	0.5
Fe-sil-1000-HT	32.0	30.4	10.8	9.4	12.2	9.7	3.4	3.00
Fe-Sil-2500-C	24.6	30.6	5.7	10.2	9.8	7.5	1.4	2.5
Fe-sil-2500-HT	47.4	18.9	16.4	15.3	22.4	9.0	7.8	7.3
Fe-sil-5000-C	34.7	16.5	14.0	17.3	26.8	5.7	4.9	6.0
Fe-sil-5000-HT	54.5	13.3	9.5	13.0	48.3	7.2	5.2	7.1

$T = 540$ °C, $m_{cat} = 200$ mg, $F = 100$ ml/min, $C_3H_8/NH_3/O_2/N_2O = 5/5/5/5$ vol.%, TOS = 15 min, nd—not detected.

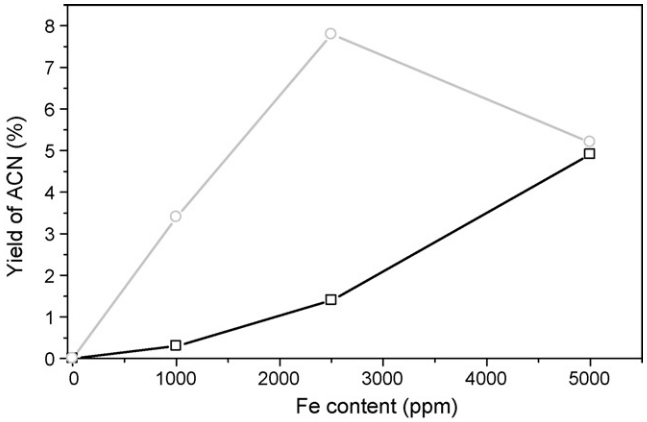

Fig. 3. Dependence of acrylonitrile yield on the concentration of Fe ions in the catalyst and on the pretreatment of the catalysts. Reaction condition: m_{cat} = 200 mg, F = 100 ml/min, T = 540 °C, TOS = 50 min, $C_3H_8/NH_3/N_2O/O_2$ = 5/5/5/5 vol.%. Calcined samples—black curve, steamed samples—gray curve.

5000-HT, for which the selectivity is slightly decreasing. Conversely, the selectivity to propene rapidly decreases from 60 to 13%. The level of propane degradation to carbon oxides is relatively low and the selectivity to CO_x does not exceed 25% for all samples with exception of Fe-sil-5000-HT, which exhibits selectivity to CO_x of 48%. The ability of investigated catalysts to produce acrylonitrile can be illustrated by dependence of ACN yield on the Fe content and pretreatment (see Fig. 3). It is evident that the activity of calcined samples is not negligible and ACN yield of calcined samples monotonically increases up to 5%. There is a generally accepted fact that only extra-framework Fe ions are responsible for redox activity of Fe catalysts [36,39]. The production of ACN by calcined samples is in agreement with the intensity of UV–vis spectra of calcined samples at 275 nm and with presence of signals with effective g-value $g \approx 8.76$ in the ESR spectra of calcined samples (cf. Figs. 1 and 2). Steam activation of Fe-silicalites led to complete extraction of Fe ions from framework position and redistribution of Fe ions in the samples, which led to increase both propane conversion and ACN selectivity. At the highest Fe concentration, steaming of catalyst enhances the process of Fe ions clustering, leading up to the formation of Fe_2O_3 nanoparticles reflected by UV–vis bands above 400 nm and broad signal at $g \approx 2.06$. ACN yield obtained over steamed samples exhibits distinct maximum at sample with 2500 ppm of iron. The drop of ACN yield for Fe-sil-5000-HT can be ascribed to massive clustering of Fe caused decrease in population isolated extra-framework Fe ions and increase in over-oxidation activity of sample due to presence oxidic particles leading to sharp increase of CO_x selectivity (see Table 1).

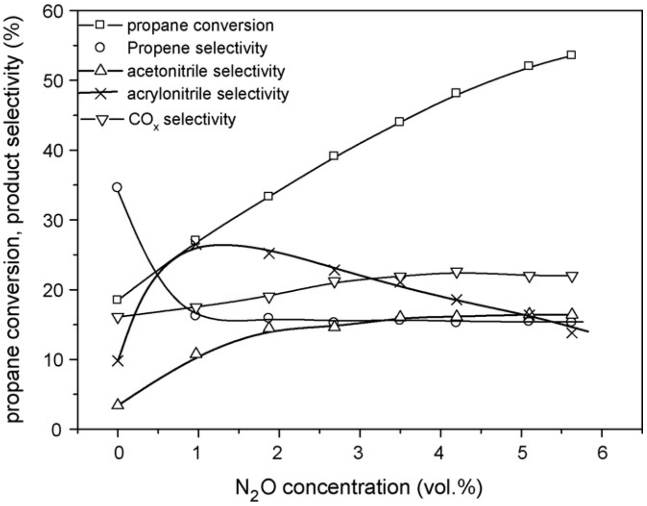

Fig. 4. Effect of variation of N_2O concentration on the catalytic performance of Fe-sil-2500-HT catalyst. Reaction condition: m_{cat} = 200 mg, F = 100 ml/min, T = 540 °C, TOS = 50 min, $C_3H_8/NH_3/O_2/N_2O$ = 5/5/5/0–6 vol.%.

As reported in literature [29,30], co-feeding of nitrous oxide and oxygen as the oxidant led to a significant increase of conversion of propane as well as the selectivity to ACN with comparison to the experiments with individual oxidants. The synergy effect of N_2O and O_2 led to minimally five-fold higher ACN yield than in the individual oxidant, when the N_2O/O_2 ratio equal 5/5 was used. However, effect of N_2O/O_2 ratio on the catalytic performance was not reported in literature. Therefore we studied the catalytic activity dependence of Fe-sil-2500-HT catalyst in the propane ammoxidation on concentration of nitrous oxide and oxygen in the reaction mixture. Fig. 4 displays the plot of propane conversion and main products selectivity as a function of N_2O concentration. The activity of catalysts in the propane ammoxidation by oxygen is relatively low. The conversion of propane reached 18% with the selectivity to ACN 9.8%. Addition only 1 vol.% of N_2O led to dramatic increase in ACN selectivity from 9.8 to 27% accompanied by sharp drop of propene selectivity from 33 to 17%. Additional increasing of N_2O concentration led to slow decrease in ACN selectivity, while propene selectivity remains unchanged. Selectivity to AcCN and CO_x slightly increases up to 2 vol.% of N_2O in the reaction mixture and then level-off. The conversion of propane monotonically increases with increasing concentration of nitrous oxide. This data clearly showed that even small amount of N_2O in the reaction mixture dramatically influenced the catalytic performance of Fe-silicalites. This positive effect of N_2O can be explained by facilitation of Fe ions re-oxidation. It is well known that N_2O oxidize Fe ions much better than molecular oxygen and special type of nascent oxygen, called alpha-oxygen, with special properties is created on Fe ions in zeolites [39–41]. Recently, the changes in the average oxidation state of nickel molybdates and vanadium oxide catalysts in the presence of N_2O were reported [42–44]. In addition, Fe-zeolites exhibit high activity in oxidative dehydrogenation of propane in the presence of N_2O [19,21–28]. If we accept general suggestion that reaction mechanism of direct ammoxidation of propane involves dehydrogenation of propane to propene in the first step, it is possible that even small amount of N_2O in the reaction mixture accelerates the activation of propane and formation of propene as an intermediate of ammoxidation reaction. However, both N_2O concentration and propane conversion can affect the products distribution in the investigated reaction. Therefore, we compared the selectivity to products in the reaction mixture with 0 and 1 vol.% of N_2O at the same conversion of propane since highest changes in the ACN selectivity were found out in these mixtures. Weight of catalyst was changed in order to obtain the same propane conversion in the mixture with 1 vol.% of N_2O as in the oxygen only (conversion was equal 18%). The ACN selectivity was 9.8 and 23.0%, AcCN selectivity was 3.4 and 8.5% and propene selectivity was 33 and 25.5% in the mixture with 0 and 1 vol.% of N_2O, respectively. It is clearly seen that the presence of nitrous oxide in the reaction mixture affects not only the activity of the catalysts but also their selectivity.

One of the advantages of steam-activated catalysts in direct ammoxidation of propane, reported by Perez-Ramirez et al. [29], is the stability of the catalyst performance in time-on-stream for 125 min. We confirm the stability of this system for at least 400 min [30]. This is in contrast to deactivation of these catalysts in propane oxidative dehydrogenation or benzene hydroxylation due to coke formation [19,26,28,36,45]. Fig. 5A and B shows the

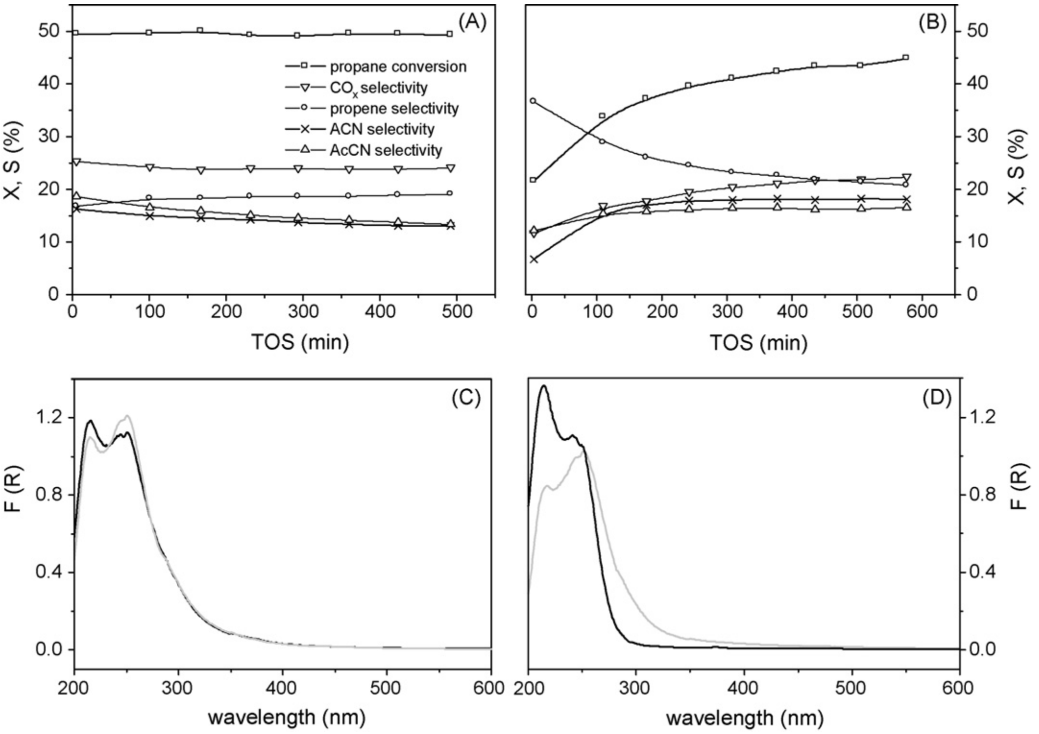

Fig. 5. Effect of time-on-stream on the catalytic behavior of Fe-sil-2500 catalysts and on distribution of Fe ions in the samples. Reaction condition: m_{cat} = 200 mg, F = 100 ml/min, T = 540 °C, $C_3H_8/NH_3/N_2O/O_2$ = 5/5/5/5 vol.%. (A) Catalytic performance of Fe-sil-2500-HT catalyst. (B) Catalytic performance of Fe-sil-2500-C catalyst. DR UV–vis spectra of hydrated Fe-sil-2500 catalysts before (black ones) and after (gray ones) catalytic run (TOS = 600 min). (C) Spectra of Fe-sil-2500-HT catalysts. (D) Spectra of Fe-sil-2500-C catalysts.

dependence of propane conversion and main products selectivity vs. time-on-stream for calcined and steamed Fe-sil-2500 catalyst. It is clearly seen that performance of steamed catalysts is stable for 8 h in good agreement with previous results, but performance of calcined sample dramatically changes during the reaction. The propane conversion increases from initial value 22 to 45% during 10 h of reaction accompanied by increasing of selectivity to ACN from 6.6 to 18% resulting to increase of ACN yield from 1.5 to 8.1%. Similarly, increase in AcCN selectivity was found. On the contrary, selectivity to propene is decreasing from 37 to 20%. This behavior of calcined catalysts is explained by intensive extraction of Fe ions in calcined sample during the reaction. This suggestion is evidenced by comparison of UV–vis spectra of sample after and before reaction. Spectra of used catalysts, measured after calcination of sample in dry oxygen at 540 °C for 1 h followed by rehydration in the air, are shown in Fig. 5C and D. It is evident that spectra of steamed samples are not notably changed but spectra of calcined samples differ significantly. Spectrum of used Fe-sil-2500-C catalyst exhibits significant increase in the intensity of bands above 275 nm at the expense of bands at 215 and 249 nm. No intensity was observed above 350 nm. This observation can be interpreted as an extraction of Fe ions from the framework and formation mainly isolated octahedral Fe ions with low population of oligomeric clusters. It means that reaction conditions (temperature of 540 °C and presence of strong ligand as ammonia and water) are sufficient for extraction and redistribution of Fe ions and effective creation of active sites for direct ammoxidation of propane. In addition, these results indicate that isolated Fe ions are the possible active centers for propane ammoxidation.

4. Conclusion

A series of Fe-silicalite catalysts with tailored dispersion of Fe sites ranging from almost exclusively isolated Fe ions via oligonuclear cluster to Fe_2O_3 particles were studied by UV–vis and ESR spectroscopy. The same catalysts were tested in the direct ammoxidation of propane and obtained catalytic results were compared with spectroscopic ones. The presented results clearly showed, that the changes in the catalytic performance of investigated catalysts are in correspondence with results of spectroscopic characterization. Main conclusions can be summarized as follows:

(1) Production of ACN increase with increasing content of extra-framework Fe ions characterized by UV–vis band at 275 nm and ESR signals with effective g-value above 5.
(2) Steam-treatment, as well as treatment of the catalysts in the reaction mixture under reaction conditions, led to extraction of isomorphously substituted Fe ions into extra-framework positions. Steam-treatment of Fe-silicalites at 600 °C in the stream of water vapor is accompanied by formation of clusters with higher number of Fe–O–Fe bonds. This has a negative impact on the selectivity of ammoxidation reaction due to high oxidation activity of oxidic cluster leading to over-oxidation of propane.
(3) Treatment of catalysts under milder conditions of ammoxidation reaction is more effective for creation of active sites. Under these conditions, the formation of oligomeric clusters and oxide nanoparticles, characterized by UV–vis bands above 300 nm and by broad ESR signals at $g \approx 2$, is prevented.
(4) Presence of even small N_2O concentration led to dramatic increase in activity of Fe-silicalites and their selectivity to acrylonitrile. This synergy effect can be postulated as a facilitation of re-oxidation of Fe centers acting in ammoxidation of propane. In addition, formation of so called alpha-oxygen enhances activation of propane and accelerates formation of propene.

Acknowledgements

The authors thank for financial support to the Grant Agency of the Czech Republic under project 104/07/0214 and Ministry of Education, Youth and Sports under the projects MSM 0021627501 and LC 512.

References

[1] H.F. Rase, Handbook of Commercial Catalysis, CRC Press, New York, 2000.
[2] J.L. Callahan, B. Gertisser, US Patent 3 198 750, 1965.
[3] G. Centi, S. Perathoner, F. Trifiro, Appl. Catal. A-Gen. 157 (1997) 143.
[4] V.D. Sokolovskii, A.A. Davydov, O.Y. Ovsitser, Catal. Rev.-Sci. Eng. 37 (1995) 425.
[5] S. Albonetti, G. Blanchard, P. Burattin, S. Masetti, F. Trifiro, 3rd World Congress on Oxidation Catalysis, Stud. Surf. Sci. Catal., vol. 110, 1997, p. 403.
[6] J. Nilsson, A.R. Landa-Canovas, S. Hansen, A. Andersson, 3rd World Congress on Oxidation Catalysis, Stud. Surf. Sci. Catal., vol. 110, 1997, p. 413.
[7] Y.C. Kim, W. Ueda, Y. Morooka, Catal. Today 13 (1992) 673.
[8] Y.C. Kim, W. Ueda, Y. Morooka, Appl. Catal. 70 (1991) 189.
[9] Y.C. Kim, W. Ueda, Y. Morooka, Chem. Lett. (1989) 2173.
[10] G. Minow, K.H. Schnabel, G. Ohlmann, React. Kinet. Catal. Lett. 22 (1983) 399.
[11] Y. Li, J.N. Armor, Appl. Catal. A-Gen. 188 (1999) 211.
[12] Y. Li, J.N. Armor, Appl. Catal. A-Gen. 183 (1999) 107.
[13] Y. Li, J.N. Armor, Abstr. Pap. Am. Chem. Soc. 216 (1998) U294.
[14] Y.J. Li, J.N. Armor, J. Catal. 176 (1998) 495.
[15] Y.J. Li, J.N. Armor, J. Catal. 173 (1998) 511.
[16] Y.J. Li, J.N. Armor, Chem. Commun. (1997) 2013.
[17] S.B. Derouane-Abd Hamid, G. Centi, P. Pal, E.G. Derouane, Top. Catal. 15 (2001) 161.
[18] S. Hamid, P. Pal, H.Y. He, E.G. Derouane, Catal. Today 64 (2001) 129.
[19] O. Sanchez-Galofre, Y. Segura, J. Perez-Ramirez, J. Catal. 249 (2007) 123.
[20] J. Perez-Ramirez, A. Gallardo-Llamas, Appl. Catal. A-Gen. 279 (2005) 117.
[21] A. Gallardo-Llamas, C. Mirodatos, J. Perez-Ramirez, Ind. Eng. Chem. Res. 44 (2005) 455.
[22] J. Perez-Ramirez, A. Gallardo-Llamas, C. Daniel, C. Mirodatos, Chem. Eng. Sci. 59 (2004) 5535.
[23] E.V. Kondratenko, J. Perez-Ramirez, Appl. Catal. A-Gen. 267 (2004) 181.
[24] J. Perez-Ramirez, A. Gallardo-Llamas, J. Catal. 223 (2004) 382.
[25] J. Perez-Ramirez, E.V. Kondratenko, Chem. Commun. (2003) 2152.
[26] R. Bulanek, J. Adam, K. Novoveska, Z. Sobalik, B. Wichterlova, Molecular Sieves: From Basic Research to Industrial Applications, Pts a and B, Stud. Surf. Sci. Catal., Vol. 158, Elsevier Science Bv, Amsterdam, 2005, p. 1977.
[27] K. Novoveska, R. Bulanek, B. Wichterlova, Catal. Today 100 (2005) 315.
[28] R. Bulanek, B. Wichterlova, K. Novoveska, V. Kreibich, Appl. Catal. A-Gen. 264 (2004) 13.
[29] J. Perez-Ramirez, N. Blangenois, P. Ruiz, Catal. Lett. 104 (2005) 163.
[30] R. Bulanek, F. Castek, Top. Catal. 45 (2007) 233.
[31] J. Perez-Ramirez, M.S. Kumar, A. Bruckner, J. Catal. 223 (2004) 13.
[32] A. Zecchina, M. Rivallan, G. Berlier, C. Lamberti, G. Ricchiardi, Phys. Chem. Chem. Phys. 9 (2007) 3483.
[33] M. Schwidder, W. Grunert, U. Bentrup, A. Bruckner, J. Catal. 239 (2006) 173.
[34] S. Bordiga, R. Buzzoni, F. Geobaldo, C. Lamberti, E. Giamello, A. Zecchina, G. Leofanti, G. Petrini, G. Tozzola, G. Vlaic, J. Catal. 158 (1996) 486.
[35] J. Perez-Ramirez, F. Kapteijn, A. Bruckner, J. Catal. 218 (2003) 234.
[36] P. Kubanek, B. Wichterlova, Z. Sobalik, J. Catal. 211 (2002) 109.
[37] B. Wichterlova, L. Kubelkova, P. Jiru, D. Kolihova, Collect. Czech. Chem. Commun. 45 (1980) 2143.
[38] B. Wichterlova, P. Jiru, React. Kinet. Catal. Lett. 13 (1980) 197.
[39] G.I. Panov, A.K. Uriarte, M.A. Rodkin, V.I. Sobolev, Catal. Today 41 (1998) 365.
[40] A.S. Kharitonov, T.N. Aleksandrova, G.I. Panov, V.I. Sobolev, G.A. Sheveleva, E.A. Paukshtis, Kinet. Catal. 35 (1994) 270.
[41] A.S. Kharitonov, V.I. Sobolev, G.I. Panov, Kinet. Catal. 30 (1989) 1319.
[42] E.V. Kondratenko, O. Ovsitser, J. Radnik, M. Schneider, R. Kraehnert, U. Dingerdissen, Appl. Catal. A-Gen. 319 (2007) 98.
[43] O. Ovsitser, M. Cherian, E.V. Kondratenko, J. Phys. Chem. C 111 (2007) 8594.
[44] F. Dury, M.A. Centeno, E.M. Gaigneaux, P. Ruiz, Appl. Catal. A-Gen. 247 (2003) 231.
[45] D.P. Ivanov, V.I. Sobolev, G.I. Panov, Appl. Catal. A-Gen. 241 (2003) 113.